Optics Communications 285 (2012) 59–63

Contents lists available at SciVerse ScienceDirect

Optics Communications

journal homepage: www.elsevier.com/locate/optcom

Efficient high-power UV laser generated by an optimized flat–flat actively Q-switched laser with extra-cavity harmonic generations

Y.J. Huang, P.Y. Chiang, H.C. Liang, K.W. Su, Y.F. Chen *

Department of Electrophysics, National Chiao Tung University, Hsinchu, Taiwan

ARTICLE INFO

Article history:
Received 30 June 2011
Accepted 2 September 2011
Available online 17 September 2011

Keywords:
Diode-pumped solid-state laser
Acousto-optically Q-switching
Parasitic lasing effect
Extra-cavity second and third harmonic generation

ABSTRACT

We investigate the parasitic lasing effect in the high-power actively Q-switched laser with a flat–flat resonator. The parasitic lasing effect in the low-Q stage is found to lead to long tails in the output pulses, corresponding to the peak-power reduction. We experimentally determine the shortest cavity length without the parasitic lasing effect to optimize the performance of the high-power actively Q-switched laser with a flat–flat cavity. We further use the optimized fundamental laser to generate green and UV lasers by extra-cavity harmonic generations. At a pump power of 44 W, the output powers at 355 nm and 532 nm as high as 6.65 W and 8.38 W are obtained at a pulse repetition rate of 40 kHz.

1. Introduction

In recent years, ultraviolet (UV) light sources have been rapidly developed because they are useful in many applications such as rapid prototyping, laser printing, laser processing, spectroscopy, optical data storage, medical treatment and so on. Compared with other UV lasers, diode-pumped all-solid-state lasers with extra-cavity harmonic generations intrinsically possess advantages of smaller focused size, higher efficiency, longer life time, higher stability, easier implement and smaller system size etc [1, 2]. The acousto-optic (AO) Q-switch is characterized by its low-insertion loss that is suitable for repetitively Q-switched lasers [3–10]. It can provide a high-stability, low timing jitter and large-peak-power laser operation with a continuously adjustable pulse repetition rate, which is beneficial for efficient extra-cavity harmonic generations.

The parasitic lasing means that there is residual lasing in the low-Q stage. The parasitic lasing effect is a critical issue for scaling up the output peak powers of the Q-switched lasers [3, 11–13]. The parasitic lasing effect of the AO Q-switched laser usually leads to a peak-power reduction that significantly deteriorates the performance of extra-cavity second and third harmonic generations (SHG and THG). Although lengthening the cavity length can effectively assist the diffraction loss of the AO device to suppress the parasitic lasing in the low-Q stage, a long cavity length usually needs an intricate design to obtain a stable resonator under the thermal lensing effect. More importantly, longer cavity lengths always lead to longer pulse widths that also reduce the output peak powers. Therefore, it is practically valuable to optimize the peak power by designing the shortest cavity length for the AO Q-switched laser without the parasitic lasing effect.

In this work, we firstly employ a Nd:YVO_4 crystal with dopant concentration as low as 0.1 atm.% in an actively Q-switched laser to explore the parasitic lasing effect in a flat–flat resonator. Experimental results reveal that the parasitic lasing leads to a long tail in the Q-switched pulse. We experimentally determine the critical cavity length without the parasitic lasing effect as a function of incident pump power. We also confirm that Nd:YVO_4 crystals with dopant concentration greater than 0.2 atm.% are hardly serviceable in designing the high-power Q-switched laser without parasitic lasing. Furthermore, we utilize the optimized laser to achieve highly efficient extra-cavity harmonic generations. At a pump power of 44 W, the output powers at 532 nm and 355 nm under a pulse repetition rate of 40 kHz reach 8.38 W and 6.65 W, respectively. The optical-to-optical conversion efficiencies from 1064 nm to 355 nm and from 808 nm to 355 nm are found to be up to 38.2% and 15.1%, respectively. To our knowledge, this is the highest conversion efficiency based on the AO Q-switched laser with a flat–flat cavity.

2. Optimization in the flat–flat AO Q-switched laser

The experimental setup is schematically shown in Fig. 1. The flat front mirror was antireflection (AR) coated at 808 nm on the entrance face, and was coated at 808 nm for high transmission as well as 1064 nm for high reflection on the second surface for lights with normal incidence. The flat folded mirror had the same coated characteristics as the flat front mirror except that the angle of the incident light was 45°. The gain medium was a 0.1 at.% Nd:YVO_4 crystal with

* Corresponding author at: Department of Electrophysics, National Chiao Tung University, 1001 TA Hsueh Road, Hsinchu, Taiwan, 30050. Fax: +886 35725230.
E-mail address: yfchen@cc.nctu.edu.tw (Y.F. Chen).

0030-4018/$ – see front matter © 2011 Elsevier B.V. All rights reserved.
doi:10.1016/j.optcom.2011.09.002

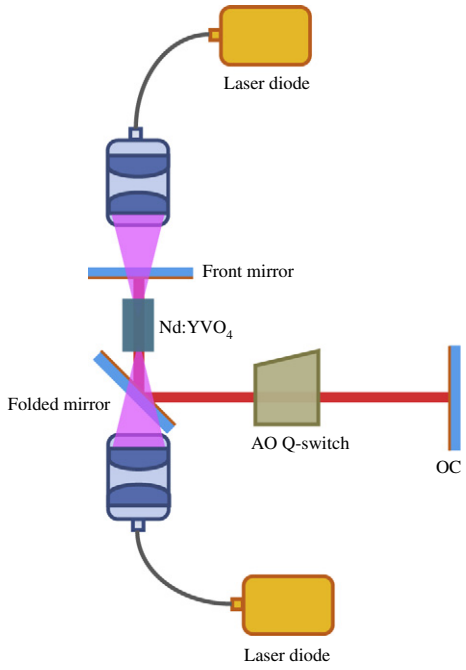

Fig. 1. Schematic of the cavity setup for a diode-pumped AO Q-switched Nd:YVO_4 laser.

dimensions of $3\times3\times14$ mm^3. Both facets of the laser crystal were AR coated at 808 nm and 1064 nm. The laser crystal was wrapped with indium foil and mounted in a water-cooled copper heat sink at 20 °C. A 20-mm-long AO Q-switch (NEOS technologies) with AR coating at 1064 nm on both faces was placed in the center of the cavity, and was driven at a central frequency of 41 MHz with RF power of 25 W. The pump sources were two 25-W 808-nm fiber-coupled laser diodes with a core diameter of 800 μm and a numerical aperture of 0.16. The pump beam was re-imaged into the laser crystal with a lens set that has the focal length of 25 mm with a magnification of unity and the coupling efficiency of 88%. As a result, the maximum pump power in our experiment is approximately 44 W. The flat output coupler with 50% transmission was employed during the experiment. The relatively low reflectance of the output coupler is practically helpful for the effective hold-off in the low-Q stage. The pulse temporal behaviors were recorded by a LeCroy digital oscilloscope (Wavepro 7100, 10 G samples/s, 1 GHz bandwidth) with a fast Si photodiode.

Since the parasitic lasing in the low-Q stage can be utterly suppressed with increasing the cavity length in a flat–flat cavity, we define the critical cavity length to be the shortest cavity length without parasitic lasing. Fig. 2 depicts experimental results for the critical

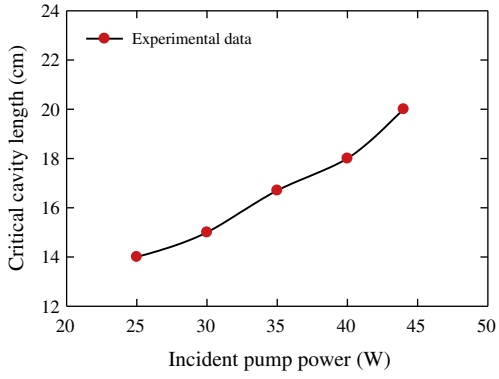

Fig. 2. Experimental results for the relationship between the critical cavity length and the incident pump power.

cavity length as a function of the pump power. The critical cavity length without parasitic lasing can be seen to increase with increasing the incident pump power. More importantly, we experimentally found that the parasitic lasing significantly affects the temporal shape of the Q-switched pulse. Fig. 3(a) and (b) shows the influence of parasitic lasing on the Q-switched pulse at the maximum pump power of 44 W for the cavity lengths of 16 cm and 18 cm, respectively. It can be seen that the Q-switched pulse is accompanied with a long tail or a satellite pulse. In contrast, the Q-switched pulse without parasitic lasing displays a short tail as well as no satellite pulse, as shown in Fig. 3(c) and (d) for the cavity lengths of 20 cm and 22 cm, respectively.

The long tail of Q-switched pulses induced by parasitic lasing implies the reduction of the peak power. The degree of the peak-power reduction can be simply analyzed with the rate equation. Assume the average photon density caused by parasitic lasing to be ϕ_b, the rate equation for the population inversion density n in the low-Q stage can be described as

$$\frac{dn}{dt}=R_p-\frac{n}{\tau}-c\sigma\phi_b n, \tag{1}$$

where R_p is the rate of the pump density, τ is the upper-state lifetime of laser crystal, c is the speed of light, σ is the stimulated emission cross section. With $\tau_b=1/c\sigma\phi_b$, Eq. (1) can be rewritten as

$$\frac{dn}{dt}=R_p-\frac{n}{\tau_e}, \tag{2}$$

where $1/\tau_e=1/\tau+1/\tau_b$ and τ_e represents the effective upper-state lifetime with parasitic lasing. τ_e is clear to be smaller than τ. Since the amount of the maximum stored energy is proportional to the upper-state lifetime, the parasitic lasing can be comprehended to cause a reduction in the pulse energy and peak power. To be brief, the parasitic lasing scarcely affects the average output power but has a detrimental effect on the peak power.

As shown in Fig. 2, the critical cavity length is approximately 20 cm for the maximum pump power of 44 W. With the ABCD-matrix theory, it can be derived that the cavity length L of a stable flat–flat resonator should be shorter than the thermal focal length f_{th},; namely, the criterion of $L\le f_{th}$ must be satisfied to maintain the cavity stable. Since the thermal focal length of the laser crystal can be verified to be inversely proportional to the dopant concentration, the criterion of $L\le f_{th}$ signifies the importance of using a Nd:YVO_4 crystal with extremely low dopant concentration. The effective focal length of thermal lens in the end-pumped laser crystal can be analyzed with the following equation [14]:

$$\frac{1}{f_{th}}=\frac{\xi P}{\pi K_c}\int_0^l\frac{\alpha e^{-\alpha z}}{1-e^{-\alpha l}}\frac{1}{\omega_p^2(z)}\left[\frac{1}{2}\frac{dn}{dT}+(n-1)\alpha_T\frac{\omega_p(z)}{l}\right]dz, \tag{3}$$

where ξ is the fraction of incident pump power that results in heat, P is the absorbed pump power, K_c is the thermal conductivity of laser crystal, α is the absorption coefficient, $\omega_p(z)$ is the variation of pump radius, dn/dT is the thermal-optic coefficient, n is the refractive index, α_T is the thermal expansion coefficient, and l is the length of gain medium. With the following parameters: $K_c=5.23$ W/m K, $\omega_{po}=400$ μm, $dn/dT=3\times10^{-6}$ K^{-1}, $n=2.1652$, $\alpha_T=4.43\times10^{-6}$ K^{-1}, we calculated the effective thermal focal length f_{th} as a function of the Nd dopant concentration of laser crystal at the incident pump power of 44 W. In the present calculation, the crystal length l is related to the absorption coefficient α with the condition of $\alpha l=4$ for pump absorption of 98%. Note that the relation between the absorption coefficient α and the Nd dopant concentration of laser crystal for a pump wavelength of 808 nm is given by $\alpha=2\cdot N_d$ mm^{-1} [15], where N_d is the Nd dopant concentration in units of atomic %. Fig. 4 depicts the calculated results ranging from $N_d=0.05\%$ to $N_d=1\%$ at

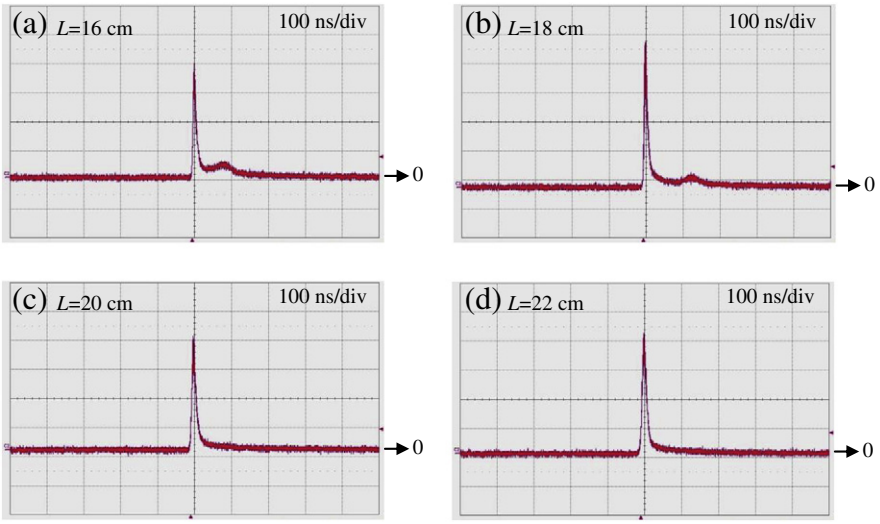

Fig. 3. Temporal behaviors of the Q-switched pulses with different cavity lengths L: (a) $L=16$ cm; (b) $L=18$ cm; (c) $L=20$ cm; (d) $L=22$ cm.

a pump power of 44 W. It can be seen that the smaller the Nd dopant concentration, the longer the thermal focal length. Moreover, the Nd:YVO_4 crystal with dopant concentration greater than 0.2 atm.% cannot comply with the requirement of $L \leq f_{th}$, where $L=20$ cm is employed to suppress the parasitic lasing at a pump power of 44 W. To sum up, using a Nd:YVO_4 crystal with extremely low dopant concentration is a promising way to simultaneously suppress the parasitic lasing and maintain a stable flat–flat resonator in high-power Q-switched lasers.

With the cavity length of 20 cm, we make a thorough evaluation for the performance of Q-switched operation. Fig. 5 shows the output power and pulse width as a function of the incident pump power at the pulse repetition rate of 40 kHz. At a pump power of 44 W, the average output power of 17.5 W was obtained without any signature of output power saturation, indicating the cavity to remain in a stable region. For the pump power increasing from 16 W to 44 W, the pulse width can be seen to decrease from 36 ns to 12 ns. Fig. 6(a) and (b) illustrates the dependences of average output power, pulse width, pulse energy and peak power on the pulse repetition rate at a pump power of 44 W. It can be seen that with increasing the pulse repetition rate from 20 kHz to 100 kHz, the average output power increases from 13 W to 19.4 W and the pulse duration smoothly varies from 8 ns to 24 ns. Accordingly, it can be found that when the pulse repetition rate increases from 20 kHz to 100 kHz, the pulse energy changes from 650 μJ to 194 μJ and the peak power varies from 81.5 kW to 8.1 kW. In the following section, we employ this compact high-power actively Q-switched laser to investigate the performance of the extra-cavity SHG and THG.

3. Performance of extra-cavity SHG and THG

Here lithium triborate (LBO) crystals are exploited as nonlinear frequency converters for SHG and THG since they have the advantages of high damage threshold, relatively large acceptance angle, and small walk-off angle. One LBO crystal with dimensions of $3\times3\times15$ mm^3 was cut at $\theta=90°$, $\varphi=10.4°$ for type-I phase-matched SHG at a temperature of 46.6 °C. Both facets of the SHG crystal were AR coated at 1064 nm and 532 nm. Another LBO crystal with dimensions of $3\times3\times10$ mm^3 was cut at $\theta=44°$, $\varphi=90°$ for type-II phase-matched THG at a temperature of 48 °C. Both facets of the THG crystal were AR coated at 1064 nm, 532 nm, and 355 nm. The temperatures of the SHG and THG nonlinear crystals were monitored by thermoelectric controllers with the precision of 0.1 °C. Two convex lenses were used to focus the laser beams into the SHG and THG nonlinear crystals for achieving efficient harmonic generations. The former one with focal length of 38 mm was AR coated at 1064 nm on both sides, the latter one with focal length of 19 mm was AR coated at 1064 nm and 532 nm on both sides. The optimized geometrical distances of L_1, L_2, L_3 and L_4 indicated in Fig. 7 were experimentally determined to be approximately 70 mm, 43 mm, 34 mm, and 21 mm, respectively.

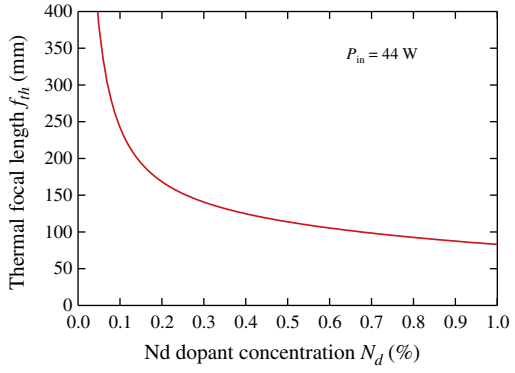

Fig. 4. Calculated results for the thermal focal length as a function of the Nd dopant concentration of laser crystal at a pump power of 44 W.

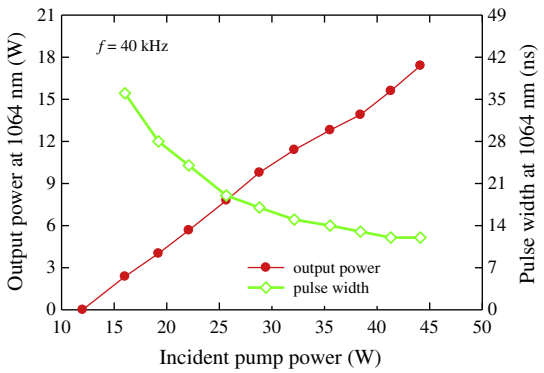

Fig. 5. Output power (red) and pulse width (green) versus the pump power at a pulse repetition rate of 40 kHz.

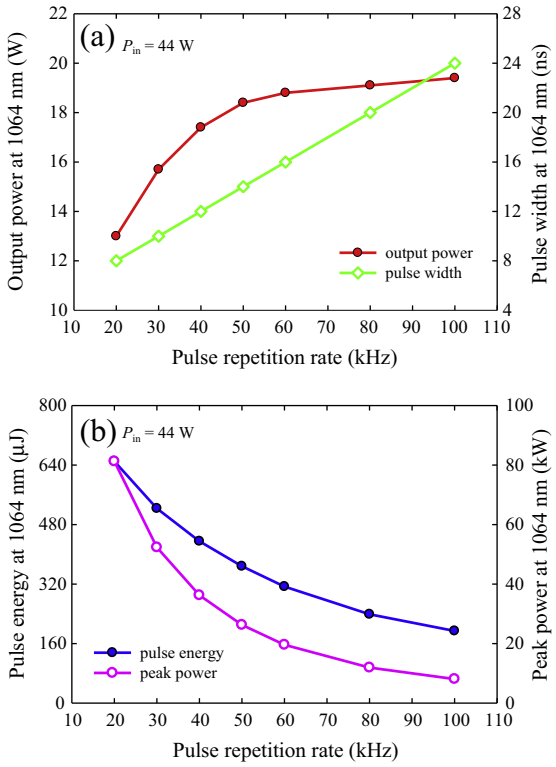

Fig. 6. (a) Dependences of the average output power (red) and the pulse width (green) on the pulse repetition rate at a pump power of 44 W; (b) dependences of the pulse energy (blue) and the peak power (pink) on the pulse repetition rate at a pump power of 44 W.

At a pump power of 44 W, the output power, the pulse energy, and the peak power at 532 nm and 355 nm versus the pulse repetition rate are shown in Fig. 8(a)–(c), respectively. Although the conversion efficiency of harmonic generations increases with decreasing the pulse repetition rate, the average output power at 1064 nm is proportional to the pulse repetition rate in the range of 20–50 kHz. As a result, the highest average output powers for extra-cavity SHG and THG are found to be approximately at a pulse repetition rate of 40 kHz and their values at 532 nm and 355 nm are 8.38 W and 6.65 W, respectively. The corresponding optical-to-optical conversion efficiencies from 808 nm to 355 nm and 1064 nm to 355 nm are up to 15.1% and 38.2%, respectively. On the other hand, at a pulse repetition rate of 20 kHz the largest pulse energy and the highest peak power at 532 nm are found to be 270 μJ and 30 kW, respectively. Similarly, at a pulse repetition rate of 20 kHz the largest pulse energy and the highest peak power at 355 nm are found to be 200 μJ and 22 kW, respectively. With a knife-edge method, the beam quality factors for orthogonal direction

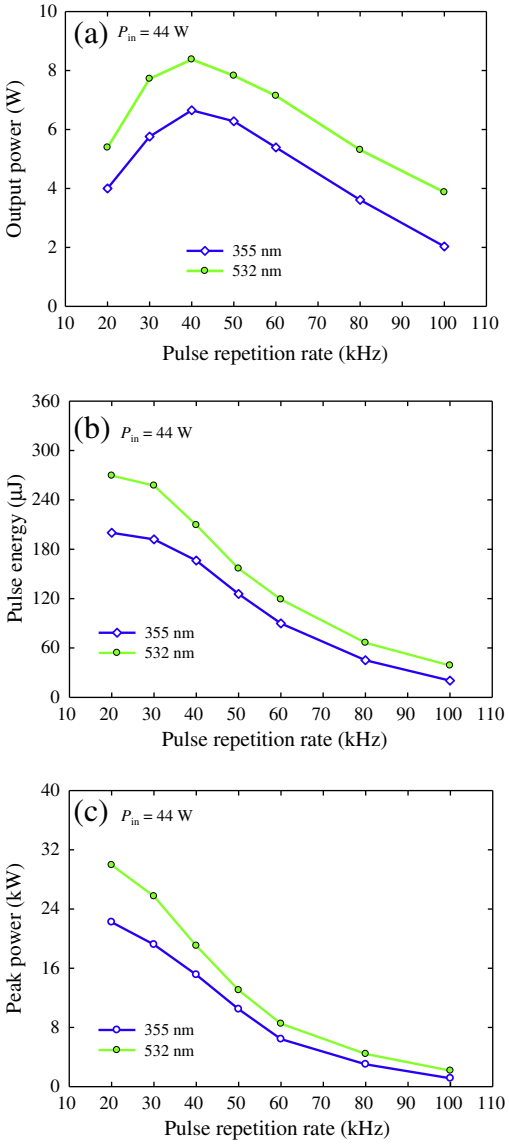

Fig. 8. Dependences of (a) the average output powers, (b) the pulse energies, and (c) the peak powers at 532 nm and 355 nm on the pulse repetition rate at a pump power of 44 W.

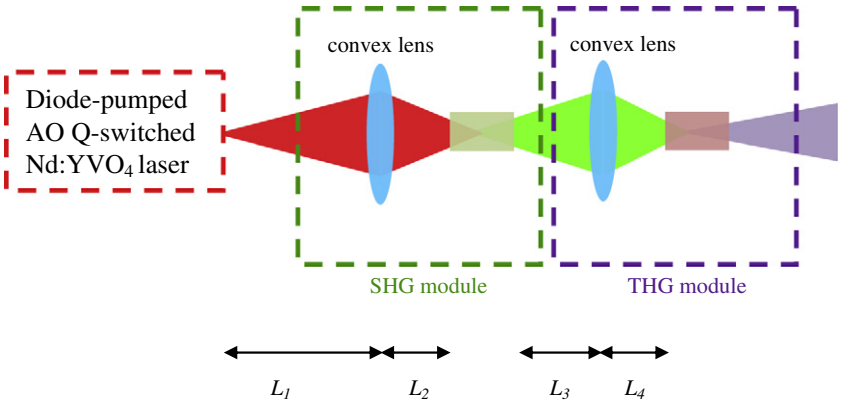

Fig. 7. Schematic of the experimental setup for the extra-cavity SHG and THG.

were measured to be $M_x^2 < 1.2$ and $M_y^2 < 1.3$. To manifest the influence of parasitic lasing on the extra-cavity harmonic generations, the Q-switched laser with $L = 16$ cm was also employed to perform the process of SHG and THG. Experimental results reveal that even though the average output power at 1064 nm obtained with $L = 16$ cm is nearly the same as that obtained with $L = 20$ cm, the average output powers at SHG and THG obtained with $L = 16$ cm were found to be 15–25% lower than the results obtained with $L = 20$ cm. The lower conversion efficiencies obtained with $L = 16$ cm confirm that the parasitic lasing effect leads to the peak-power reduction in Q-switched lasers.

4. Conclusion

In summary, we have explored the parasitic lasing effect in an actively Q-switched laser with a flat–flat resonator and a 0.1 atm.% Nd:YVO_4 crystal. Experimental results revealed that the critical cavity length without parasitic lasing was proportional to the pump power. The parasitic lasing effect was also found to lead to a long tail in the Q-switched pulse, corresponding to a reduction in the peak power. We manifestly disclosed that the combined effects of the parasitic lasing and the thermal lensing made Nd:YVO_4 crystals with dopant concentration greater than 0.2 atm.% to be problematical in designing the high-power Q-switched laser with a flat–flat cavity. We further employed the optimized high-power Q-switched laser without parasitic lasing to achieve highly efficient extra-cavity harmonic generations. At a pump power of 44 W, the output powers at 355 nm and 532 nm as high as 6.65 W and 8.38 W are obtained at the pulse repetition rate of 40 kHz. The optical-to-optical conversion efficiencies from 1064 nm to 355 nm and 808 nm to 355 nm are up to 38.2% and 15.1%, respectively.

Acknowledgments

The authors thank the National Science Council for their financial support of this research under contract no. NSC-97-2112-M-009-016-MY3.

References

[1] A.V. Hicks, C.X. Wang, G.Y. Wang, Proceedings of SPIE 5332 (2004) 120.
[2] C.X. Wang, G.Y. Wang, A.V. Hicks, D.R. Dudley, H.Y. Pang, N. Hodgson, Proceedings of SPIE 6100 (2006) 610019.
[3] P. Maak, L. Jakab, P. Richter, H.J. Eichler, B. Liu, Applied Optics 39 (2000) 3053.
[4] J. Liu, C. Wang, C. Du, L. Zhu, H. Zhang, X. Meng, J. Wang, Z. Shao, M. Jiang, Optics Communications 188 (2001) 155.
[5] J.H. García-López, V. Aboites, A.V. Kir'yanov, M.J. Damzen, A. Minassian, Optics Communications 218 (2003) 155.
[6] T. Ogawa, T. Imai, K. Onodera, H. Machida, M. Higuchi, Y. Urata, S. Wada, Applied Physics B 81 (2005) 521.
[7] Li Shutao, Zhang Xingyu, Wang Qingpu, Cong Zhenhua, Liu Zhaojun, Fan Shuzhen, Zhang Xiaolei, Journal of Physics D: Applied Physics 41 (2008) 055104.
[8] Su Fufang, Zhang Xingyu, Wang Qingpu, Ding Shuanghong, Jia Peng, Li Shutao, Fan Shuzhen, Zhang Chen, Liu Bo, Journal of Physics D: Applied Physics 39 (2006) 2090.
[9] F. He, L. Huang, M. Gong, Q. Liu, X. Yan, Laser Physics Letters 4 (2007) 511.
[10] X. Li, X. Yu, F. Chen, R. Yan, J. Gao, J. Yu, D. Chen, Optics Express 17 (2009) 9468.
[11] M.E. Storm, Journal of the Optical Society of America B 9 (1992) 1299.
[12] T. Crawford, C. Lowrie, J.R. Thompson, Applied Optics 35 (1996) 5861.
[13] P. Yan, M. Gong, T. Xie, X. Liu, Optical Engineering 42 (2003) 159.
[14] W. Koechner, Solid-State Laser Engineering, 6th ed. Spring-Verlag, Berlin, Germany, 2005 ch. 7.
[15] Y.F. Chen, IEEE Quantum Electronics 35 (1999) 234.